Anal. Chem. **2006,** *78,* 6990−6998

Subsecond Voltammetric Separation between Dopamine and Serotonin in the Presence of Ascorbate

Costas A. Anastassiou,*,†,‡ Bhavik A. Patel,‡ Martin Arundell,‡ Mark S. Yeoman,§ Kim H. Parker,‡ and Danny O'Hare‡

Institute of Biomedical Engineering and Department of Bioengineering, Imperial College London, Prince Consort Road, SW7 2AZ, London, UK, and Therapeutics and Pharmacology, School of Pharmacy and Biomolecular Sciences, University of Brighton, Cockcroft Building, Moulsecoomb, Brighton, East Sussex BN2 4GJ, UK

Downloaded via UNIV OF BRIGHTON on March 10, 2021 at 10:37:01 (UTC).
See https://pubs.acs.org/sharingguidelines for options on how to legitimately share published articles.

Although voltammetry has proved an important tool for unraveling the dynamics of specific neurotransmitter molecules during the past decade, it has been very difficult to monitor more than one neurotransmitter simultaneously. In this work, we present a voltammetric methodology that allows discrimination between dopamine and serotonin, two important neurotransmitter molecules with very similar electrochemical properties, in the presence of high concentrations of ascorbate. We combined the application of a novel large-amplitude/high-frequency voltage excitation with signal processing techniques valid for the analysis of nonstationary and nonlinear phenomena. This allows us to minimize the contribution from capacitance and preserve the faradaic features of the voltammetric response providing us with excellent voltammetric detail. Using appropriate voltage excitation parameters and defining specific regions in the voltage space, so-called voltage windows, we can measure the concentrations of dopamine and serotonin separately or independently in mixed solutions even in the presence of high concentrations of ascorbate. Because of the enhanced voltammetric detail of this new technique, it is also possible to explore effects attributed to interfacial phenomena such as adsorption/desorption and electrode fouling.

There have been many studies of the role of neurotransmitters in different physiological or pathological states ranging from detailed investigations of the physiology of neurotransmission to the effects of drug addiction and its relation to behavior and activity.[1−6] In many of these studies, voltammetry using ultramicroelectrodes (electrodes of typically less than 10 μm) has emerged as the method of choice offering unparalleled spatial and temporal resolution combined with submicromolar sensitivity.[7,8]

The majority of neurotransmitter studies using voltammetry have been restricted to the detection of only one neurotransmitter, typically dopamine, although important work has been done to allow the simultaneous measurement of a single neurotransmitter with other species, for instance, dopamine and oxygen.[9] The release of dopamine can be stimulated from selective CNS regions such as the striatum that is known to contain the terminals of dopaminergic neurons.[10] On the other hand, cumulative studies using microdialysis coupled with either liquid chromatography or capillary electrophoresis have reported the presence of a number of neurotransmitters coexisting in specific regions of the brain in a variety of organisms.[11−14] Furthermore, multiple neurotransmitters have been measured not only from specific brain regions but also from individual neurons. For example, Kennedy and Jorgenson[15] and Kennedy et al.[16] measured the neurotransmitter content from three individual neurons in the snail *Helix aspersa* and found femtomolar levels of dopamine, serotonin, tyrosine, and tryptophan. To investigate subsecond changes in such systems and understand their role and interaction during pharmacological and behavioral studies, it is important to develop methods capable of detecting more than one neurotransmitter within the biological matrix.

* To whom correspondence should be addressed. E-mail: c.anastassiou@imperial.ac.uk.

† Institute of Biomedical Engineering, Imperial College London.

‡ Department of Bioengineering, Imperial College London.

§ University of Brighton.

(1) Staal, R. G. W.; Mosharov, E. V.; Sulzer, D. *Nat. Neurosci.* **2004**, *7*, 341−346.

(2) Wang, C. T.; Grishanin, R.; Earles, C. A.; Chang, P. Y.; Martin; T. F. J.; Chapman, E. R.; Jackson, M. B. *Science* **2001**, *294*, 1111−1115.

(3) Heien, M. L. A. V.; Khan, A. S.; Ariansen, J. L.; Cheer, J. F.; Phillips, P. E. M.; Wassum, K. M.; Wightman, R. M. *Proc. Natl. Acad. Sci. U.S.A.* **2005**, *102*, 10023−10028.

(4) Sombers, L. A.; Ewing, A. G. In *Electroanalytical Methods for Biological Materials*; Brajter-Toth, A., Chambers, J. Q., Eds.; Marcel Dekker: New York, 2002; pp 279−327.

(5) Cannon, D. M.; Winograd, N.; Ewing, A. G. *Annu. Rev. Biophys. Biomol.* **2000**, *29*, 239−263.

(6) Joseph, J. D.; Wightman, R. M. In *Electroanalytical Methods for Biological Materials*; Brajter-Toth, A., Chambers, J. Q., Eds.; Marcel Dekker: New York, 2002; pp 255−278.

(7) Wightman, R. M. *Anal. Chem.* **1981**, *53*, 1125−1128.

(8) Wightman, R. M. *Science* **2006**, *311*, 1570−1574.

(9) Zimmerman, J. B.; Wightman, R. M. *Anal. Chem.* **1991**, *63*, 24−28.

(10) Stamford, J. A.; Kruk, Z. L.; Millar, J.; Wightman, R. M. *Neurosci. Lett.* **1984**, *51*, 133−138.

(11) Westerink, B. H. C. *TRAC, Trends Anal. Chem.* **1992**, *11,* 182−186.

(12) Lu, J.; Zhang, S.; Wang, A.; Zhang, W.; Jin, L. *Talanta* **2000**, *52*, 807−815.

(13) Patel, B. A.; Arundell, M.; Parker, K. H.; Yeoman, M. S.; O'Hare D. *J. Chromatogr., B* **2005**, *818*, 269−276.

(14) Jung, M. C.; Shi, G.; Borland, L.; Michael, A. C.; Weber, S. G. *Anal. Chem.* **2006**, *78*, 1755−1760.

(15) Kennedy, R. T.; Jorgenson, J. W. *Anal. Chem.* **1989**, *61*, 436−441.

(16) Kennedy, R. T.; Oates, M. D.; Cooper, B. R.; Nicerson, B.; Jorgenson, J. W. *Science* **1989**, *246*, 57−63.

10.1021/ac061002q CCC: $33.50 © 2006 American Chemical Society
Published on Web 08/25/2006

There are two strategies for obtaining selectivity in voltammetry: selection of the appropriate applied voltage or engineering the electrode surface using selective membranes.[17,18] Among the many possible voltammetric methodologies, fast scan cyclic voltammetry (FSCV), which uses a ramp as the excitation voltage, has been predominantly used to minimize the perturbation of biological concentrations, electrode fouling, adrenochrome formation, etc.[19] Additionally, the measurement of neuronal activity requires the application of rapid voltage waveforms that provide the subsecond and submillisecond temporal resolution that FSCV can offer. However, the larger the voltage perturbation gradients, the larger the contribution of capacitance to the electrode current becomes, which increases the difficulty in characterizing the electrochemical response and thus the underlying dynamics. This is also observed for FSCV where capacitance due to double layer charging significantly distorts the current response at typical scan rates.[3,8,17]

To separately measure neurotransmitters such as dopamine (DA) and serotonin (5-HT), a number of issues have to be addressed. The major difficulty is that DA and 5-HT possess a very similar FSCV current response and an oxidation potential (E_0) separation of less than 150 mV (E_0(DA) = 200 mV and E_0-(5-HT) = 320 mV versus Ag|AgCl), making them difficult to discriminate.[20] The distortion of the electrochemical signature of the neurotransmitters by capacitance contributions further complicates the process of their discrimination. Additionally, in many mammalian preparations, such as the rat striatum, high concentrations of ascorbate (AA) are present, typically 100−1000 μM, and cannot be neglected. AA poses an important complication of in vivo and in vitro electroanalysis (i) because of its contribution to the total current[21] and (ii) by chemically reacting with oxidized neurotransmitters, their intermediates, or both (see Supporting Information).[22] Selective coatings and electrochemical pretreatment of the electrodes can ameliorate the electrochemical contribution of AA to some extent, but permselective films increase response times and the effects of electrochemical activation/pretreatment are short-lived.[23−25]

The significant capacitance interference caused by rapid voltage excitations is typically dealt with by application of background subtraction either in situ (background is recorded prior to evoked release) or from recordings of the signal in buffer.[3,26,27] This is problematic for two reasons: (i) it assumes that the background current is independent of the faradaic reaction; (ii) the charging current can be as much as 2 orders of magnitude larger than the faradaic signal. The assumption of a constant background is not justified, especially where the faradaic reaction involves adsorbed intermediates and proton transfers, which can cause changes in local pH. The enormous difference in relative magnitude of frequently noisy signals can undermine the validity of the subtraction process, and the subtraction of large currents from small signals can also lead to digitization errors.

Another method that has been used in the past to overcome the effect of capacitance and relate specific patterns of the current response to the underlying dynamics is based on the fast Fourier transform (FFT). Ac voltammetry, which consists of a voltage ramp upon which is superimposed a harmonic voltage excitation, typically a few millivolts to minimize nonlinear contributions, was combined with FFT to discriminate capacitance contributions, mainly present in the fundamental harmonic of the ac spectrum, from other processes.[17] Recently, large-amplitude/high-frequency ac voltammetry was shown to combine a number of attractive features such as the possibility to interrogate process dynamics on different time scales, explore the kinetics and thermodynamics of different processes, or selectively target specific process dynamics, such as parallel reactions.[28] It is due to these features that large-amplitude/high-frequency ac voltammetry, from this point simply referred to as ac voltammetry, has been applied to systems as diverse as inorganic out-of-sphere electron-transfer and surface-immobilized proteins.[29,30]

The disadvantage in using ac voltammetry in combination with an FFT-based analysis is that Fourier techniques assume periodicity and linearity whereas transient voltammetric data are inherently nonstationary and nonlinear. A nonlinear process does not obey the principle of superposition, nor does it have the property of frequency preservation.[31] An alternative signal processing technique that has been used for the analysis of nonstationary and nonlinear processes is the Hilbert transform (HT).[32] The HT has been typically used to calculate the instantaneous attributes of time-domain signals in phenomena ranging from the synchronization characteristics of neurons to changes in pulmonary blood pressure.[33,34]

We have shown recently that the instantaneous amplitude of the analytic signal calculated using the HT allows minimization of the nonfaradaic contributions by means of a simple offset.[35,36] Furthermore, it allows direct continuous assessment of time-dependent changes in the capacitance signal. In this paper, we show how ac voltammetry combined with the HT can be used to effectively discriminate between DA and 5-HT through judicious selection of voltage excitation regions, the so-called "voltage window", and optimization of the excitation waveform parameters.

(17) Bard, A. J.; Faulkner, L. R. *Electrochemical Methods*, 2nd ed.; Wiley: New York, 2001.
(18) Wiedemann, D. J.; Bassetomusk, A.; Wilson, R. L.; Rebec, G. V.; Wightman, R. M. *J. Neurosci. Methods* **1990**, *35*, 9−18.
(19) Martin, K. F.; Marsden, C. A.; Crespi, F. *TRAC, Trends Anal. Chem.* **1988**, *7*, 334−339.
(20) Kovach, P. M.; Ewing, A. G.; Wilson, R. L.; Wightman, R. M. *J. Neurosci. Methods* **1984**, *10*, 215−227.
(21) Tse, D. C. S.; McCreery, R. L.; Adams, R. N. *J. Med. Chem.* **1976**, *19*, 37−40.
(22) Venton, B. J.; Troyer, K. P.; Wightman, R. M. *Anal. Chem.* **2002**, *74*, 539−546.
(23) Gerhardt, G. A.; Oke, A. F.; Nagy, G.; Moghaddam, B.; Adams, R. N. *Brain Res.* **1984**, *290*, 390−395.
(24) Kovach, P. M.; Ewing, A. G.; Wilson, R. L.; Wightman, R. M. *J. Neurosci. Methods* **1984**, *10*, 215−227.
(25) Pihel, K.; Walker, Q. D.; Wightman, R. M. *Anal. Chem.* **1996**, *68*, 2084−2089.
(26) Williams, G. V.; Millar, J. *Neuroscience* **1990**, *39*, 1−16.
(27) Millar, J.; O'Connor, J. J.; Trout, S. J.; Kruk, Z. L. *J. Neurosci. Methods* **1992**, *43*, 109−118.
(28) Bond, A. M.; Duffy, N. W.; Guo, S. X.; Zhang, J.; Elton, D. *Anal. Chem.* **2005**, *77*, 186A−195A.
(29) Sher, A. A.; Bond, A. M.; Gavaghan, D. J.; Harriman, K.; Feldberg, S. W.; Duffy, N. W.; Guo, S. X.; Zhang, J. *Anal. Chem.* **2004**, *76*, 6214−6228.
(30) Fleming, B. D.; Barlow, N. L.; Zhang, J.; Bond, A. M.; Armstrong, F. A. *Anal. Chem.* **2006**, *78*, 2948−2956.
(31) Director, S. W.; Rohrer, R. A. *Introduction to system theory*; McGraw-Hill: New York, 1972.
(32) Gabor, D. *Proc. IEE* **1946**, *93*, 429−457.
(33) Siapas, A. G.; Lubenov, E. V.; Wilson, M. A. *Neuron* **2005**, *46*, 141−151.
(34) Huang, W.; Shen, Z.; Huang, N.; Fung, Y. C. *Proc. Natl. Acad. Sci. U.S.A.* **1998**, *96*, 1834−1839.
(35) Anastassiou, C. A.; Parker, K. H.; O'Hare, D. *Anal. Chem.* **2005**, *77*, 3357−3364.
(36) Anastassiou, C. A.; Ducros, N.; Parker, K. H.; O'Hare, D. *Anal. Chem.* **2006**, *78*, 4383−4389.

The latter not only serves to increase the neurotransmitter current response relative to the capacitance but also minimizes the influence of AA in our analysis. We have used voltage excitation waveforms that are able to negate any faradaic features of AA in the presence of neurotransmitters. The enhanced voltammetric detail gained using this new methodology allows changes due to adsorption/desorption phenomena and electrode fouling to be followed in real time.

MATERIALS AND METHODS

Chemicals. AA, DA, and 5-HT were obtained from Sigma-Aldrich and used as received. Solutions were prepared in 10 mM phosphate-buffered saline (PBS) buffer (138 mM NaCl and 2.7 mM KCl) pH 7.4. Stock analyte solutions were prepared in PBS buffer pH 7.4.

Electrode Preparation. Electrode fabrication was based on the work by Millar and Pelling.[37] The 7-μm carbon fibers were sonicated in acetone for 15 min, cleaned in methanol and deionized water, and dried using nitrogen. Glass capillaries (0.69-mm i.d., Clark Electromedical Instruments, Reading, UK) were pulled using a pipet puller (model PP-830, Narishige, Tokyo, Japan), and then the tips were polished on emery paper to facilitate the insertion of the carbon fiber. The capillaries where then rinsed with ethanol and deionized water and dried in nitrogen. The carbon fiber was threaded through the pulled end of the glass capillaries. Once the carbon fiber was inserted, it was sealed within the capillary using epoxy resin (CY1301 epoxy resin and HY1300 hardener; Robnor Resins Ltd., Swindon, Wilts, UK). Drying and curing took 72 h at room temperature. Connection was achieved by contacting a 0.25-mm silver wire using Woods metal. The exposed tip of the carbon fiber was cut to an approximate length of 2 mm before the shaft of the fiber was insulated using nail polish (Revlon, France). The carbon fiber was then cut using a scalpel to expose a 7 μM carbon disk electrode.

Experimental Analysis of DA and 5-HT. DA and 5-HT solutions of bulk concentration ranging from 1 to 20 μM were produced from the stock solution and diluted using PBS buffer containing 500 μM AA. Experiments were carried out in the three-electrode configuration where the reference electrode was a Ag|AgCl wire in a 3 M KCl solution (CHI Instruments), the counter electrode was an in-house platinum flag electrode, and the working electrode the 7-μm carbon fiber disk microelectrode. The ramped harmonic waveforms were digitally generated using Labview 7.0 software (National Instruments, Austin, TX) and converted to an analog signal through a NI PCI 6036E card interfaced with a custom-built potentiostat, which was also used to record the current output signal (16-bit, 200-kHz bandwidth).

Flow Cell Experiments. The flow cell was fabricated using a Sylgard silicone elastomer, using a ratio of 10:1 (v/v) of base to curing agent. A mold was created using two pipet tips as holders for the counter and reference electrodes, and a channel was created by using 1.6-mm HPLC PEEK tubing. End-column detection was used for the working electrode. A HPLC connector was placed at the other end of the flow cell to allow for connection to the HPLC pump (HP1050, Agilent). Elastomer was poured into the mold and cured at 80 °C for 1 h. Once cured the mold was slowly cooled to room temperature and gently removed. The HPLC inlet connector was then sealed to the flow cell using Torr Seal epoxy resin.

(37) Millar, J.; Pelling, C. W. A. *J. Neurosci. Methods* **2001**, *110*, 1−8.

Experiments were carried out using a three-electrode configuration, where the working electrode was the 7-μm carbon fiber disk electrode. A stainless steel counter electrode and an in-house fabricated Ag|AgCl reference electrode were used for measurements.[38] A potential of +750 mV was used for all amperometric experiments. Calibration data were obtained for 5-HT in the concentration range of 100 nM−5 μM, carried out in continuous flow for 50 s before switching concentration. The flow rate was 5 mL min^{-1}. All experiments were carried out in PBS buffer with pH 7.4.

Hilbert Transform. In this work, we use the HT of a real-valued time series as defined by Gabor.[32] The HT of $I(t)$, $\bar{I}(t)$, is the time series that makes the complex time series $z(t) = I(t) + j\bar{I}(t)$ analytic (i.e., it satisfies the Cauchy−Riemann conditions) where j is the imaginary number. The HT of $I(t)$ can be realized in several ways, one of which is through the Cauchy integral:

$$\bar{w}(t) = HT[I(t)] = \int_{-\infty}^{\infty} \frac{I(t)}{\pi(t-u)}\,\mathrm{d}u \qquad (1)$$

The Hilbert transform is a linear operator, and it allows the calculation of the instantaneous amplitude $a_I(t)$ and the instantaneous phase $\varphi_I(t)$ of $z(t)$ from the polar form:

$$z(t) = a_I(t)e^{j\varphi_I(t)} \qquad (2)$$

Because both the $\bar{I}(t)$ and the analytic signal $z(t)$ are defined in the time domain, the HT is suitable for the analyses of nonstationary processes and has often been used to analyze nonlinear phenomena.[33,34] Moreover, it has been shown that the HT can be used to minimize the influence of capacitance on ac voltammetry data as well as to monitor electrode surface blocking.[35,36,39]

RESULTS AND DISCUSSION

The methodology introduced in this paper uses the ac voltammetry voltage excitation, which is the superposition of a "slow" dc signal with a large-amplitude/high-frequency harmonic signal in order to obtain an electrochemical signature from the two analytes of interest, DA and 5-HT. In Figure 1A, we show the applied voltage E versus time t where the dc scan rate $v = 2$ V s^{-1}, the amplitude of the large-amplitude/high-frequency harmonic oscillation $\Delta E = 0.4$ V, the driving-frequency $f^* = 150$ Hz, and the initial voltage $E_{in} = -0.1$ V. The current response I of an ac voltammetry experiment from a 50 μM DA solution in a PBS buffer containing 500 μM AA measured with a carbon microelectrode is shown in Figure 1B. There the presence of both the reduction and oxidation envelopes are observed at $t = 0.15$ s and $t = 0.18$ s. From the current output signal I shown in Figure 1B, we calculate the instantaneous amplitude a_I of the analytic signal $z(t)$ using the HT and the result is shown in Figure 1C. By comparing a_I versus t (Figure 1C) with I versus t (Figure 1B), it is observed that the envelopes due to the faradaic response are preserved while the capacitance contributions are substantially minimized. Because of the minimization of capacitance, it is also easier to

(38) Cater, D. B.; Silver, I. A. *Reference Electrodes*; Ives, D. G., Ives, G. J., Eds.; Academic Press: London, 1961.

(39) Arundell, M.; Patel, B. A.; Yeoman, M. S; Parker, K. H.; O'Hare, D. *Electrochem. Commun*. **2004**, *6*, 366−372.

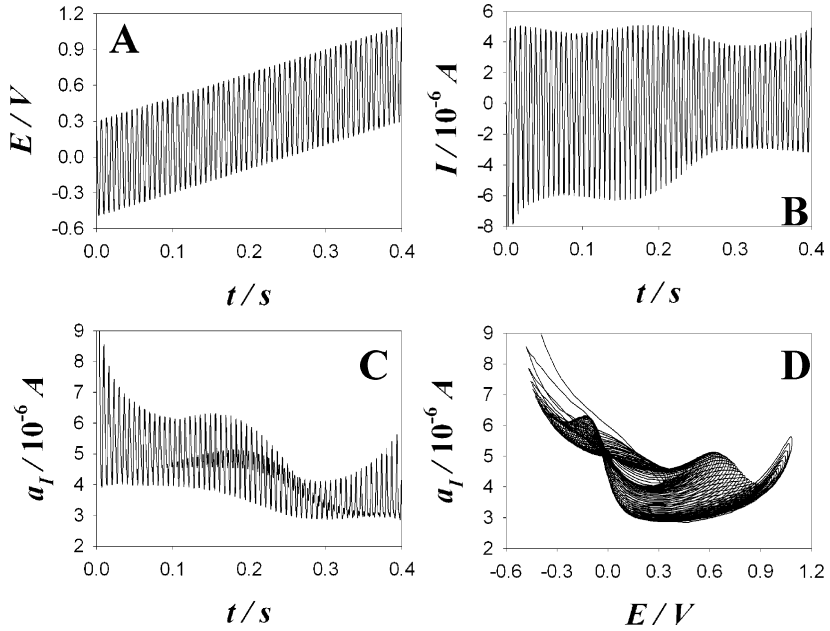

Figure 1. (A) Applied voltage E in ac voltammetry vs time t ($v = 2$ V s^{-1}, $\Delta E = 0.4$ V, and $f^* = 150$ Hz). (B) The current response I of an ac voltammetry experiment from a 50 μM DA solution in a PBS buffer containing 500 μM AA. (C) a_I of I, as calculated with the HT, vs time t. It is observed that the faradaic response is preserved while the capacitance contribution is substantially minimized (compare to (B)). (D) a_I vs E indicates the presence of the DA faradaic peaks at $E = -0.15$ and 0.60 V.

account for changes in the capacitance during the course of an experiment. Moreover, when plotting a_I versus the applied voltage E, the DA faradaic peaks at $E = -0.15$ and 0.60 V are clearly seen (Figure 1D).

The voltage excitation parameters used in Figure 1 were chosen for two reasons: (a) they offer a good time resolution, the duration of the experiment is only 0.4 s, relevant for monitoring baseline changes in neurotransmitter concentrations,[3] and (b) they provide a strong enough electrochemical signal and signal-to-noise ratio to enable measurements of micromolar and submicromolar neurotransmitter concentrations. In fact, we conducted an experimental sensitivity analysis of the voltage excitation parameter space by exploring a large number of possibilities. An example is shown in Figure 2A, where we compare the characteristic reduction envelope of a 10 μM DA solution for a "faster" (black: $v = 2$ V s^{-1}, $\Delta E = 0.4$ V, $f^* = 150$ Hz) and a "slower" excitation waveform (magenta: $v = 2$ V s^{-1}, $\Delta E = 0.3$ V, $f^* = 80$ Hz). In both cases, $E_{in} = -0.1$ V. As can be seen, the capacitance contribution is efficiently minimized to an offset in both voltammograms by the use of the HT but the faster excitation waveform offers an enhanced electrochemical response for DA.

In Figure 2B, we show that by choosing a faster excitation waveform, the influence of AA, which is present in a number of biological systems in 100−1000-fold higher concentrations than the neurotransmitter itself, significantly decreases. The a_I of a 500 μM AA solution in PBS is shown for $v = 2$ V s^{-1}, $\Delta E = 0.4$ V, and $f^* = 150$ Hz (black) and for $v = 0.2$ V s^{-1}, $\Delta E = 0.1$ V, and $f^* = 25$ Hz (magenta). While the black envelope is characteristic of purely capacitive effects, showing no signs of faradaic events, the magenta envelope shows the typical AA electrochemical response at $E = 0.6$ V. Thus, we can conclude that by using the faster excitation waveform we can minimize the interference from AA.

To test the stability of the current response, I sinusoidal voltammetry in combination with the HT analysis was used.[35,39,40] In Figure 2C and D, the results of this analysis are shown. In Figure 2C, the instantaneous amplitude of the current response a_I when the voltage excitation parameters $v = 0$ V s^{-1}, $\Delta E = 0.4$ V, $f^* = 150$ Hz, and $E_{in} = 0.3$ V of two subsequent cycles (first cycle, solid lines; second cycle, dotted lines) is illustrated at four different times: $t_1 = 0.03$ s (black), $t_2 = 0.06$ s (blue), $t_3 = 0.11$ s (cyan), and $t_4 = 0.31$ s (magenta). As can be seen, the envelopes remain stable both from cycle to cycle and throughout the duration of the experiment. This is also illustrated in Figure 2D, where the reduction (circles) and oxidation (rectangles) baseline-subtracted peak amplitudes are plotted for each cycle for two voltage excitations: $v = 0$ V s^{-1}, $\Delta E = 0.4$ V, $f^* = 150$ Hz, and $E_{in} = 0.3$ V (empty symbols) and $v = 0$ V s^{-1}, $\Delta E = 0.7$ V, $f^* = 150$ Hz, and $E_{in} = 0.3$ V (solid symbols). The slight signal attenuation with time observed for $\Delta E = 0.7$ V relative to $\Delta E = 0.4$ V is attributed to the increased rate of adsorption typically observed for fast voltage excitations that can lead to electrode blockage.

Calibration working curves were constructed in order to analyze changes in neurotransmitter concentration. The experiments are shown in Figure 3 for DA and 4 for 5-HT. The voltage excitation used for these experiments was $v = 2$ V s^{-1}, $\Delta E = 0.4$ V, $f^* = 150$ Hz, and $E_{in} = -0.1$ V. In Figure 3A and B, we show I versus t for a 15 μM DA solution and a_I versus t after application of the HT to minimize the effects of capacitance. As can be seen, changes in capacitance during the experiment can be monitored from the changes in the capacitance baseline in a_I. When plotting a_I versus E, Figure 3C, the peaks in both the reduction ($E = 0$ V) and the oxidation ($E = 0.6$ V) envelopes can be seen clearly. The amplitude of these envelopes changes systematically with solution

(40) Millar, J.; O'Connor, J. J.; Trout, S. J.; Kruk, Z. L. *J. Neurosci. Methods* **1992**, *43*, 109−118.

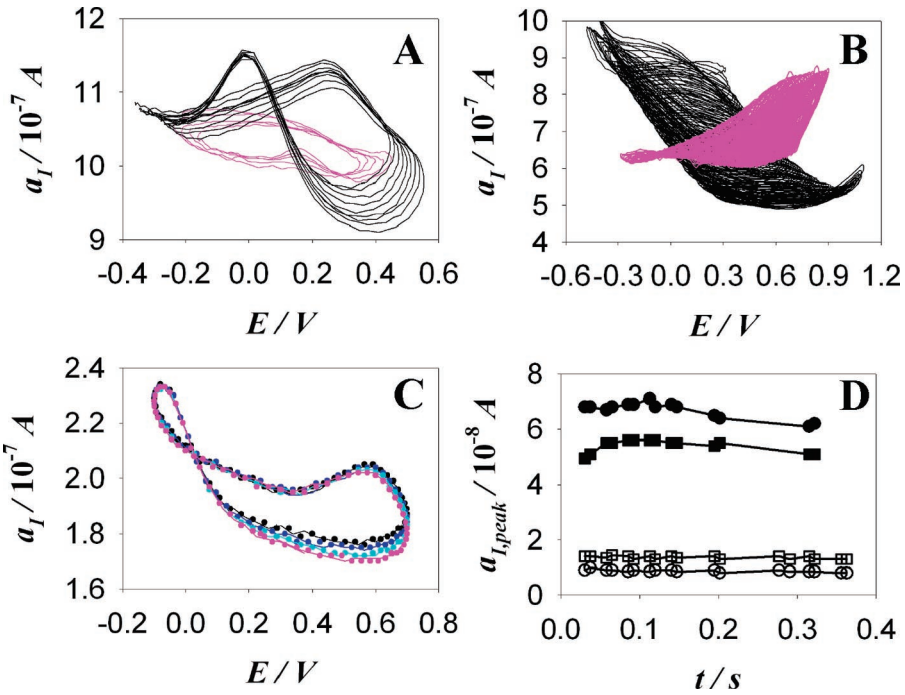

Figure 2. In (A) the characteristic reduction envelope of a 10 μM DA solution is seen in a_I as a function of E for $v = 2$ V s^{-1}, $\Delta E = 0.4$ V, and $f^* = 150$ Hz (black) and $v = 2$ V s^{-1}, $\Delta E = 0.3$ V, and $f^* = 80$ Hz (magenta). In (B), the influence of AA is larger for slower excitation waveforms with the black line indicating the response for $v = 2$ V s^{-1}, $\Delta E = 0.4$ V, and $f^* = 150$ Hz and the cyan line for $v = 0.2$ V s^{-1}, $\Delta E = 0.1$ V, and $f^* = 25$ Hz. In (C), the effect of AA on DA is studied using sinusoidal voltammetry ($v = 0$ V s^{-1}, $\Delta E = 0.4$ V, and $f^* = 150$ Hz.) The results from two subsequent cycles (first cycle, solid lines; second cycle, dotted lines) are presented for four different times: $t_1 = 0.03$ s (black), $t_2 = 0.06$ s (blue), $t_3 = 0.11$ s (cyan), and $t_4 = 0.31$ s (magenta). Variation is minimal for fast excitations as seen in (D) where the baseline-subtracted peak amplitude of the reduction (●) and the oxidation (■) currents is plotted for two sinusoidal voltammetry amplitudes: $\Delta E = 0.4$ V (empty symbols) and $\Delta E = 0.7$ V (full symbols).

concentration. To quantify these changes for DA, we used the three reduction cycles that form the peak of the reduction envelope indicated by the red circle in a_I versus E (Figure 3C). To do so, we defined a so-called "DA window" that includes these three reduction cycles and is designated by the red bars in Figure 3B and C ($E = -0.3$ V to $E = 0.4$ V). In Figure 3D, we show how the amplitude of a_I changes in the DA window for four different bulk concentrations: 15 (black), 7.5 (blue), 2.5 (cyan), and 0 μM (pure AA, magenta).

The same concept was applied to analyze different solution concentrations for 5-HT. In Figure 4A, the current response I versus t is shown in for a 20 μM 5-HT solution. The a_I versus t plot in Figure 4B indicates the presence of an oxidation ($E = 0.6$ V) and, unlike DA, a much weaker reduction envelope ($E = 0.1$ V).[20] Additionally, it is observed that the oxidation envelope of 5-HT extends to higher voltages than the DA response. Because the amplitude peaks of the oxidation waves of DA and 5-HT overlap at the DA window, compare Figures 3B and C with 4B and C, and because the purpose of this work is to develop strategies to analyze solutions where both DA and 5-HT are present, the so-called 5-HT voltage window was chosen at approximately $E = 0.1$ V to $E = 0.9$ V, indicated by the green bars, when the influence of the DA response is small. Thus, unlike for DA, the three cycles that form the oxidation envelope to be analyzed do not represent the overall envelope maximum of the oxidation envelope of 5-HT. As a result, the green circle that designates the location of the maximum value of these three oxidation cycles does not coincide with the overall maximum of the oxidation wave as seen in Figure 4C. In Figure 4D, we show how the amplitude of a_I in the 5-HT window changes for four different 5-HT solution concentrations: 20 (black), 10 (blue), 5 (cyan), and 0 μM (pure AA, magenta).

The results using the methodology introduced in Figures 3 and 4 are summarized in Figure 5, where the changes in the amplitude of a_I in the DA and 5-HT window are shown for pure solutions of DA and 5-HT at different solution concentrations in the presence of 500 μM AA in PBS. The circles, for DA, and squares, for 5-HT, represent the mean of three sensors ($n = 3$) while the bars represent ranges. There is a linear relationship between a_I and concentration of DA in the DA window for concentrations up to 10 μM. The correlation coefficient $R^2 = 0.97$. At higher concentrations, there is a decrease in sensitivity presumably due to saturation of the electrode surface by adsorbed DA.[22] Thus, the presence of 5-HT does not affect the value of the peak in the DA window. In Figure 5B, we show that DA has an effect in the 5-HT window but the DA signal is much smaller than the 5-HT signal. This is especially true for lower, and physiologically more relevant, concentrations, i.e., <5 μM, where the DA signal is ~10-fold weaker than the 5-HT signal. This is also observed in Figure 5C, where the raw data in the 5-HT window is shown for two 20 μM (black) and two 5 μM (blue) solutions, one for DA and one for 5-HT. As seen, 5-HT overwhelms the DA response in the 5-HT window, which resembles the AA, and thus the blank, response (magenta). To further suppress the DA response in the 5-HT window, an alternative would be to choose the 5-HT window for higher voltages, for example, from $E = 0.2$ V to $E = 1.0$ V. The 5-HT window $E = 0.1$ V to $E = 0.9$ V ($t = 0.3$ s) was chosen because it offers a good compromise between

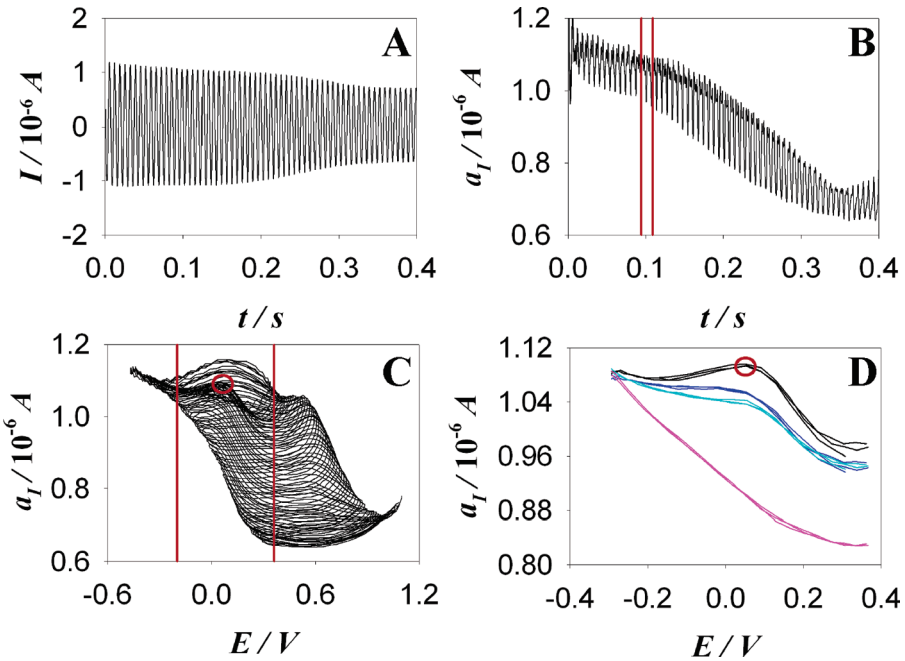

Figure 3. Analysis of the DA ac voltammetry response for different bulk concentrations of DA. (A) I vs t for a 15 μM DA solution when $v = 2$ V s^{-1}, $\Delta E = 0.4$ V, and $f^* = 150$ Hz. (B) a_I vs t after application of the HT. (C) When plotting a_I vs E, both the reduction ($E = 0$ V) and the oxidation ($E = 0.6$ V) envelopes are apparent. (D) The three reduction cycles with the largest peaks are plotted as a function of bulk concentration. The four DA bulk concentrations shown are 15 (black), 7.5 (blue), 2.5 (cyan) and 0 μM (pure AA, magenta). The so-called DA voltage window is designated by the red lines in (B) and (C) and includes three consecutive from $E = -0.3$ V to $E = 0.4$ V ($t = 0.1$ s). The red circle indicates the peak value of the oxidation envelope in the overall response in (C) and in the DA window in (D).

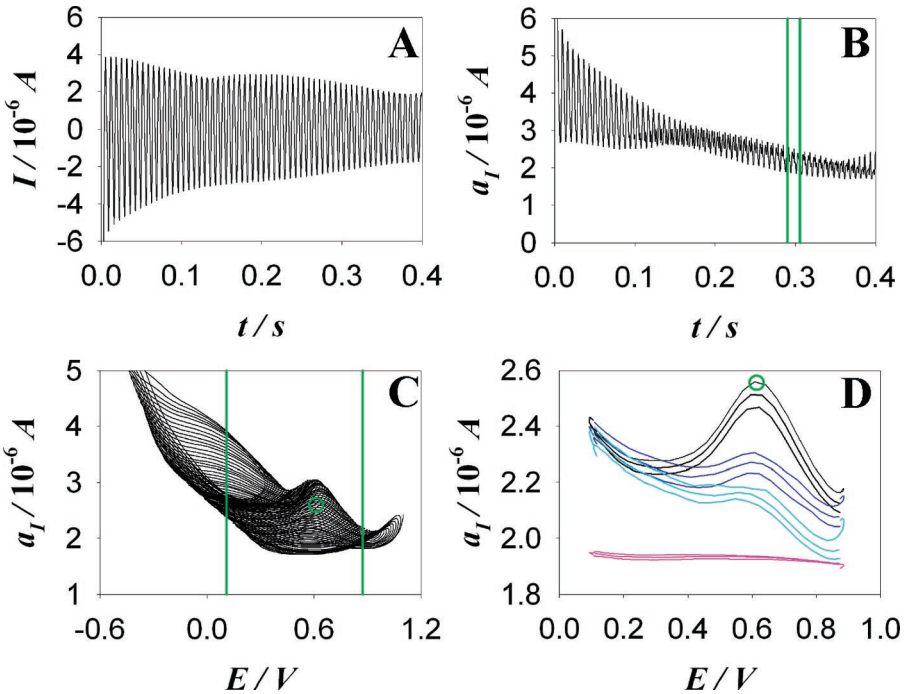

Figure 4. Analysis of the 5-HT ac voltammetry response for different bulk concentrations of 5-HT. (A) The current response I vs t for a 20 μM 5-HT solution. (B) The a_I vs t plot indicates the presence of an oxidation and a weak reduction envelope. (C) Because the envelope peaks of DA and 5-HT almost overlap (compare Figure 3B and 3C with 4B and 4C) the three consecutive cycles to be used to monitor changes in bulk concentration, the 5-HT voltage window, is chosen for 5-HT at approximately $E = 0.1$ V to $E = 0.9$ V, indicated by the green lines, where the DA response is small. Thus, unlike DA, the green circle indicating the cycles to be analyzed does not represent the overall envelope peak. (D) The four concentrations shown are 20 (black), 10 (blue), 5 (cyan), and 0 μM (pure AA, magenta).

sensitivity and selectivity. It has to be mentioned that in order to guarantee the usefulness of the methodology so-called "blind" experiments were carried out where the operator was unaware of the solution compositions. More precisely, the blind experiments involved three solutions with each neurotransmitter, DA or 5-HT ($n = 6$; concentration range, 1−15 μM). In all experiments, the operator was able to predict the neurotransmitter present within 5−10% error in concentration.

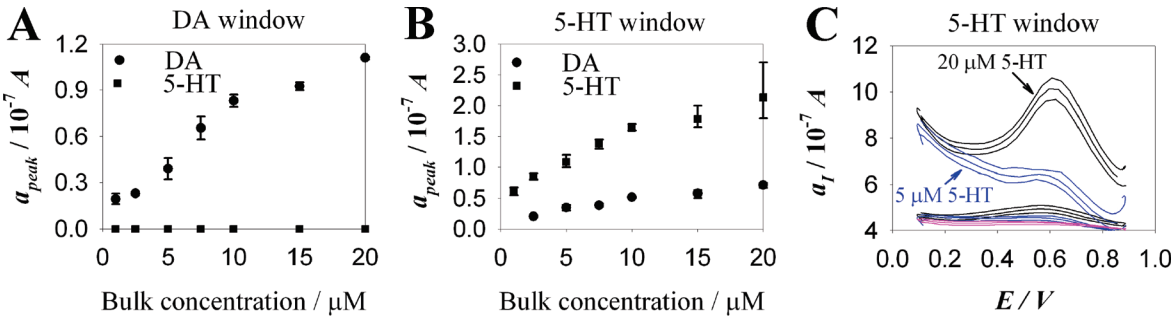

Figure 5. Peak amplitude response of purely DA or 5-HT solutions in the presence of AA and PBS as a function of bulk concentration of the neurotransmitter. Circles (for DA) and squares (for 5-HT) indicate the average of 3 electrodes; the bars indicate the range. (A) The peak amplitude response from the three consecutive cycles is shown in the DA window as a function of bulk concentration of DA and of 5-HT solutions. (B) The peak amplitude response in the 5-HT window. While there is a small influence of DA in this window, the 5-HT response is much larger, especially for bulk concentrations lower than 10 μM. (C) The responses of two 5-HT solutions in the 5-HT window are shown, a 20 μM (top black) and a 5 μM (top blue) compared to the responses from a 20 μM (lower black) and a 5 μM (lower blue) DA solution. The influence of AA is indicated by the magenta lines.

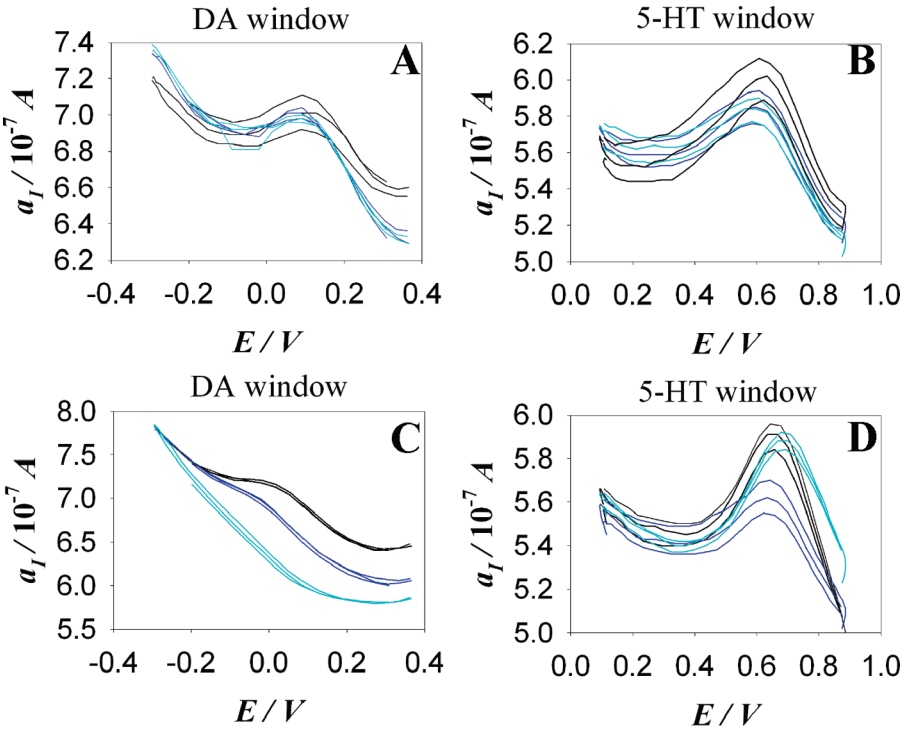

Figure 6. Analysis of solutions with both DA and 5-HT present. (A, B) The responses in the DA (A) and the 5-HT (B) window for a 5 μM DA and 1 μM 5-HT solution in the first scan (black), after 1.5 s (blue) and after 3 s (cyan). (C, D) The same responses in the DA (C) and the 5-HT (D) windows for 10 μM DA and 10 μM 5-HT solution. While the response in the 5-HT window remains overall constant, the DA response diminishes progressively, indicating the increase of 5-HT and the decrease of DA surface concentration.

In Figure 6, the analysis using the above method is shown for solutions where both DA and 5-HT are present. Two solutions were investigated: (i) a solution containing 5 μM DA and 1 μM 5-HT and (ii) a solution containing 10 μM DA and 10 μM 5-HT. In both experiments, the buffer included 500 μM AA and PBS. For both solutions, repeated measurements were conducted and here we plot a_I in the DA and the 5-HT window with the black lines indicating the initial experiment, the blue lines after 1.5 s and the cyan lines after 3 s. Plots A and B in Figure 6 show the DA and the 5-HT window for the 5 μM DA and 1 μM 5-HT solution while plots C and D show the 10 μM DA and 10 μM 5-HT solution. At the lower concentrations, first row, it is observed that the response is stable and reproducible throughout the experiment in both windows and the values of the a_I peaks correspond well to the calibration curves shown in Figure 5. At the higher concentrations, second row, it is evident that, while the response in the 5-HT window remains stable overall, the response in the DA window diminishes progressively to finally vanish completely.

Both DA and 5-HT follow an EC reaction mechanism where the molecule is adsorbed on the electrode surface before undergoing a 2-electron transfer and desorption. It has been shown experimentally that while DA and 5-HT exhibit comparable adsorption time constants, 5-HT desorbs more slowly than DA.[41,42]

(41) Jackson, B. P.; Dietz, S. M.; Wightman, R. M. *Anal. Chem.* **1995**, *67*, 1115−1121.
(42) Zhou, F.-M.; Liang, Y.; Salas, R.; Zhang, L.; De Biasi, M.; Dani, J. A. *Neuron* **2005**, *46*, 65−74.

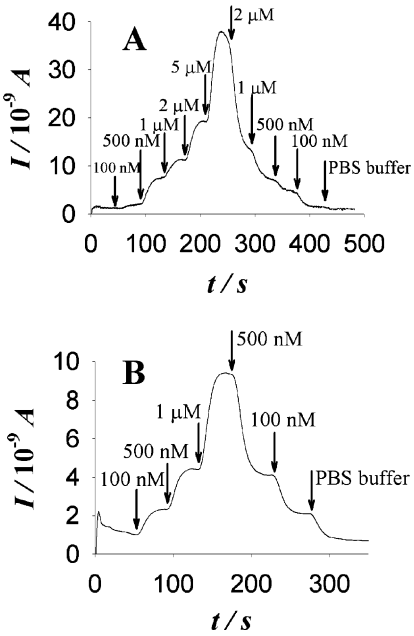

Figure 7. Amperometric recordings of 5-HT carried out for continuous flow of the analyte solution. (A) The responses for up to 5 μM 5-HT solutions are shown where the current amplitudes for the various concentrations are not symmetrical with respect to the point of symmetry at $t = 230$ s. (B) Repeating the same experiment with the maximum 5-HT concentration being 1 μM, it is observed that the current recording is symmetrical with respect to the point of symmetry at $t = 175$ s thus indicating that the electrode surface is still active. Both experiments were carried out using a fresh 7-μm disk carbon fiber microelectrode for detection at a potential of +750 mV vs Ag|AgCl.

Thus, the decreasing DA response of the higher concentration equimolar solution is attributed to progressive saturation of the electrode surface with 5-HT. On the other hand, the rate of saturation of the electrode surface is also a function of the bulk concentration.[41] For a 5-fold higher concentration of DA relative to 5-HT (Figure 6A and B), the DA peak amplitude is preserved, suggesting that the effect of bulk concentration can overcome the limitation of desorption kinetics. The results reported in Figure 6 are representative of a series of experiments with 12 solutions with both DA and 5-HT present where for 8 of them (DA:5-HT) = (2.5−20 μM, 1 μM) while for 4 of them (DA:5-HT) = (5−20 μM, 2.5−10 μM). In all of the eight experiments where the 5-HT concentration was 1 μM, the current output remained constant for the duration of the experiment, ~3.5 s. For the four experiments where the 5-HT concentration was larger the 1 μM, the electrode surface was progressively occupied by 5-HT resulting in an attenuation of the DA response.

Another important aspect of the interfacial dynamics is that 5-HT not only progressively occupies the electrode surface but may also polymerize in the oxidized form to permanently block the surface sites on the carbon electrode.[43] The attenuation of the current response due to electrode blockage, also referred to as electrode fouling, decreases with decreasing analyte flux to the electrode surface to a point below which it becomes negligible. Manica et al.[44] measured this effect on a Pt microelectrode using an electrophoresis microchip and found that the effect of fouling decreased substantially for 5-HT concentrations below 1 μM. Tostudy the concentration dependence of adsorption/blockage, detailed amperometric flow cell experiments were conducted where the working electrode was subjected to a continuous flow of the 5-HT solution at increasing and then decreasing concentrations (Figure 7). In Figure 7A, the current is shown when the maximum 5-HT concentration injected is 5 μM. It is observed that during the incremental increase of the 5-HT concentration the current increases nearly stepwise with some transient effects attributed to adsorption kinetics. The changes in concentration were performed every 50 s, which was the time needed to obtain a steady-state amperometric response. Subsequently, the concentration of the injected 5-HT was decreased in a symmetric manner and it is observed that the amperometric response does not follow the changes in concentration in a symmetrical way, having longer response times and lower asymptotes. This asymmetry in the current response (compare $t < 230$ s with $t > 230$ s) is characteristic of an almost completely fouled electrode surface indicating the presence of an insulating polymerized 5-HT film. In Figure 7B, the same experiment is repeated with a fresh electrode with the maximum 5-HT concentration being 1 μM. The shape of the amperometric response to this decreased concentration profile was very symmetrical, indicating an active electrode surface throughout the course of the experiment. Therefore, we are able to infer that 1 μM represents the 5-HT concentration above which electrode blockage occurs for the carbon fiber electrodes used in this study, as also suggested for Pt electrodes of comparable size.[44]

CONCLUSIONS

In this work, we have presented a novel voltammetric methodology that allows the subsecond separation between DA and 5-HT in the presence of the main physiological interference, AA. To do so we applied ac voltammetry where the voltage excitation is the superposition of a slower dc signal with a large-amplitude/high-frequency harmonic signal and used the HT to calculate the instantaneous amplitude of the analytic signal. This allowed us to considerably suppress the impact of capacitance and to monitor changes of the capacitance baseline throughout the experiment. We showed that the current response from the two neurotransmitters and AA can be optimized for the analyte of interest by adjusting the voltage excitation parameters. Based on the instantaneous amplitude, we defined the DA and 5-HT windows, which included three cycles of the reduction (for DA) and oxidation (for 5-HT) envelopes to discriminate between DA and 5-HT. This allowed us to quantify changes in the solution concentration up to 10 μM not only of single-component solutions but, more importantly, in solutions where the two analytes coexisted in comparable concentrations. Furthermore, we were able to track the dynamics of adsorption/desorption of the two neurotransmitters on the electrode surface as well as the occurrence of electrode fouling. We believe that this methodology can offer unprecedented temporal information regarding the presence and coexistence of DA or 5-HT in a neuronal system.

(43) Dryhurst, G. *Chem. Rev.* **1990**, *90*, 795−811.
(44) Manica, D. P.; Mitsumori, Y.; Ewing, A. G. *Anal. Chem.* **2003**, *75*, 4572−4577.

ACKNOWLEDGMENT

C.A.A. and B.A.P. thank Peiling Leow for experimental assistance. C.A.A. thanks the Institute of Biomedical Engineering and the EPSRC for financial support (Grant number: GR/R89127/01). B.A.P. is funded by an EPSRC LSI postdoctoral fellowship (Grant EP/C532058/1).

SUPPORTING INFORMATION AVAILABLE

Additional information as noted in text. This material is available free of charge via the Internet at http://pubs.acs.org.

Received for review June 1, 2006. Accepted July 25, 2006.

AC061002Q